Published in final edited form as:
Adv Funct Mater. 2020 March 03; 30(10): . doi:10.1002/adfm.201909614.

Enhanced Fluorescence for Bioassembly by Environment-Switching Doping of Metal Ions

Dr Kai Tao, **Dr Yu Chen**
School of Molecular Cell Biology and Biotechnology, George S. Wise Faculty of Life Sciences, Tel Aviv University, 6997801 Tel Aviv, Israel

Asuka A. Orr,
Artie McFerrin Department of Chemical Engineering, Texas A&M University, College Station, TX 77843-3122, USA

Dr Zhen Tian
Joint Key Laboratory of the Ministry of Education, Institute of Applied Physics and Materials Engineering, University of Macau, Avenida da Universidade, Taipa, Macau, China

Dr Pandeeswar Makam, **Dr Sharon Gilead**
School of Molecular Cell Biology and Biotechnology, George S. Wise Faculty of Life Sciences, Tel Aviv University, 6997801 Tel Aviv, Israel

Prof Mingsu Si,
Key Laboratory for Magnetism and Magnetic Materials of MOE, Key Laboratory of Special Function Materials and Structure Design, Ministry of Education, Lanzhou University, 730000 Lanzhou, China

Dr Sigal Rencus-Lazar,
School of Molecular Cell Biology and Biotechnology, George S. Wise Faculty of Life Sciences, Tel Aviv University, 6997801 Tel Aviv, Israel

Prof Songnan Qu,
Joint Key Laboratory of the Ministry of Education, Institute of Applied Physics and Materials Engineering, University of Macau, Avenida da Universidade, Taipa, Macau, China

Prof Mingjun Zhang,
Department of Biomedical Engineering, College of Engineering, The Ohio State University, Columbus, OH 43210, USA

Prof Phanourios Tamamis[*],
Artie McFerrin Department of Chemical Engineering, Texas A&M University, College Station, TX 77843-3122, USA

Prof Ehud Gazit[*]
School of Molecular Cell Biology and Biotechnology, George S. Wise Faculty of Life Sciences, Tel Aviv University, 6997801 Tel Aviv, Israel

ehudg@post.tau.ac.il; tamamis@tamu.edu.

Conflict of Interest
The authors declare no conflict of interest.

Europe PMC Funders Author Manuscripts

Abstract

The self-assembly of cyclodipeptides composed of natural aromatic amino acids into supramolecular structures of diverse morphologies with intrinsic emissions in the visible light region is demonstrated. The assembly process can be halted at the initial oligomerization by coordination with zinc ions, with the most prominent effect observed for cyclo-dihistidine (cyclo-HH). This process is mediated by attracting and pulling of the metal ions from the solvent into the peptide environment, rather than by direct interaction in the solvent as commonly accepted, thus forming an "environment-switching" doping mechanism. The doping induces a change of cyclo-HH molecular configurations and leads to the formation of pseudo "core/shell" clusters, comprising peptides and zinc ions organized in ordered conformations partially surrounded by relatively amorphous layers, thus significantly enhancing the emissions and allowing the application of the assemblies for ecofriendly color-converted light emitting diodes. These findings shed light into the very initial coordination procedure and elucidate an alternative mechanism of metal ions doping on biomolecules, thus presenting a promising avenue for integration of the bioorganic world and the optoelectronic field.

Keywords

aromatic cyclodipeptides; bioinspired LEDs; metal ion doping; supramolecular fluorescence; very initial oligomerization

1 Introduction

Bioinspired assembling materials have demonstrated promising potential to serve as the foundation for next-generation photoelectronics.[1–4] Among these materials, aromatic short peptides can self-assemble into nanostructures with remarkable photoactive features.[5–7] With extensive and directional hydrogen bonding and aromatic interactions serving as the driving forces,[8–11] aromatic short peptides can provide new frontiers of smart materials, allowing a better interface between photoactive constituents and sustainable optoelectronics. Hence, attempts are being made to utilize these properties toward developing bioorganic semiconductors.[12]

Aiming to modulate the properties and extend the applications of semiconductors, doping has been employed as an effective strategy.[13,14] For state-of-the-art organic semiconductors, the doping approaches generally include redox reactions (chemical or electrochemical) or complicated procedures (coevaporation or spin-coating), which involve relatively reactive materials or harsh experimental conditions.[15–17] In contrast, transition metal ions coordination can be utilized for peptide self-assembly, allowing the modulation of their supramolecular morphologies along with the corresponding properties in an ecofriendly manner.[18–21] For example, Zn(II) or Cu(II) coordination of the self-assembly of amyloid proteins and amyloid-like short peptides can result in structural polymorphism.[22–26] Likewise, BFPms1 (a green fluorescent protein mutant)[27] and its derived aromatic short peptide tryptophan-phenylalanine (linear-WF)[28] show high binding affinity to Zn(II) and assemble into supramolecular structures with enhanced fluorescence emission. However, although extensive efforts have been made in order to clarify the coordination mechanisms

between metal ions and peptide assemblies,[29,30] the very initial interactions between the metal ions and the peptide molecules, which guide their association into oligomeric clusters and subsequently into larger supramolecular structures underlying the molecular mechanism of photoactive features, are still elusive.

Herein, we extensively studied the self-assembly and corresponding photoluminescent properties of all 10 cyclodipeptides composed of the natural aromatic amino acids,[31–33] including histidine (H), W, F, and tyrosine (Y) (Figure S1, Supporting Information), and studied the coordination mechanism between zinc ions and cyclo-HH, which shows the most effective doping consequence and photoluminescent enhancement. We demonstrate for the first time that following doping with Zn(II), the metal ions are initially attracted and pulled from the solvent to a more peptide-rich environment, as opposed to the currently accepted notion stating that the two entities directly assemble in the solvent, thus giving rise to an "environment-switching" doping mechanism. We suggest that the coordination leads to configurational changes of the peptide molecules and promotes the peptides to assemble into pseudo "core/shell" clusters. Each cluster comprises an ordered β-bridge like conformation as the core and a relatively amorphous surrounding aggregate as the shell (Scheme 1), thereby underlying the structural mechanism for photoluminescence enhancement.

2 Results and Discussion

2.1 Aromatic Cyclodipeptide Assemblies Show Intrinsically Visible Photoluminescence

Briefly, after dissolving the cyclodipeptide powder in methanol and heating to 80 °C, most peptides were dissolved (except cyclo-FF and cyclo-YY). Atomic force microscopy (AFM) analysis demonstrated that the cyclodipeptides self-assembled into diverse architectures with dimensions ranging from dozens to hundreds of nanometers, including nanospheres (cyclo-WW),[31] nanofibers (cyclo-HH,[31] cyclo-FF, cyclo-HY, cyclo-WH, cyclo-WY, cyclo-HF, cyclo-FY) and platelets (cyclo-YY, cyclo-FW) (Table 1; Figure S2, Supporting Information). This implies that the supramolecular morphologies can be finely modulated by simply modifying the peptide residues.[34,35] High-magnification AFM revealed that alongside the larger supramolecular morphologies, nanoparticles of 2 to 10 nm were also present. For example, along with the nanofibers, discrete, dot-like nanoparticles could be detected in the cyclo-HY and cyclo-WH systems (Figure S2K,L, Supporting Information), implying the hierarchical assembly in these bio-organic architectures.[36] Thus, it could be concluded that the aromatic cyclodipeptides first oligomerize into nanodots, which comprise the intermediates to further assemble into larger nanostructures.[12,37]

Aromatic amino acids show intrinsic fluorescence with emission at 360 nm (Ex: 220 nm), 348 nm (Ex: 280 nm), 282 nm (Ex: 257 nm) and 274 nm (Ex: 220 nm) for H, W, F, and Y, respectively.[38,39] These wavelengths are all in the UV light region (<400 nm), thus severely limiting their application in biological systems and for ecofriendly photoelectronics. Density functional theory (DFT) calculations demonstrated that although the spatial distributions of the highest occupied molecular orbitals were dispersed on both the backbone diketopiperazine and the side-chain aromatic rings, the electron clouds distribution was only concentrated on the side-chain aromatic rings for the lowest unoccupied molecular orbitals of the cyclodipeptides (Figure S3, Supporting Information), indicating that the aggregations,

along with the potential photoactive properties, were mostly driven by π–π interactions between aromatic side chains.[33] Specifically, the band gaps (ΔE) were calculated to be between 3.56 and 4.55 eV (Table 1), indicating the widegap semiconducting nature of the dipeptide assemblies.[40,41]

The aromatic interactions could decrease the electron transition energy and lead to the through-space conjugation of the electron clouds, thus inducing the red shift of the assemblies.[12,33,42] The excitation-resolved emission contour profiles were studied (Figure S4, Supporting Information) and the corresponding maximal excitation (λ_{Ex}) and emission (λ_{Em}) wavelengths are summarized in Table 1. Except cyclo-YY, cyclo-FF (with no detectable emissions) and cyclo-HY (λ_{Em} at 390 nm), all other cyclo-dipeptide self-assemblies showed fluorescence of no less than 400 nm (Table 1). Notably, cyclo-HH, cyclo-WW and cyclo-WH self-assemblies showed two λ_{Em} each, namely 425 nm (Ex: 340 nm) & 520 nm (Ex: 420 nm), 440 nm & 520 nm (Ex: 370 nm),[31] and 380 nm (Ex: 320 nm) & 465 nm (Ex: 370 nm), respectively (Table 1, Figure S4A,C,F, Supporting Information). These spectroscopic findings indicated the hierarchical organization and the size-encoded photoluminescence of the assemblies, consistent with the AFM results. In addition, the photoluminescence of the self-assemblies showed remarkable stability, with fluorescence lifetimes (τ) of ≈5 ns and cyclo-WH showing the longest τ of up to 11 ns for the 465 nm emission (Table 1).

2.2 Zinc Ions Mediated Photoluminescence Enhancement

The dominant emissions of the peptide self-assemblies were between 400 and 465 nm, in the blue and blue-green region (Table 1). However, the photoluminescence efficiency of the peptide self-assemblies was low, with quantum yield (QY) of only 2–3% (with the exception of cyclo-HH, which showed a QY of 7% for the 520 nm emission) (Table 1). Aiming to increase the efficiency, Zn(II) was introduced to the aromatic cyclodipeptide solutions, thereby attempting to decrease the electron-transfer energy barrier and enhance the QY.[28] Fluorescence characterization demonstrated that the emission intensity of the cyclo-HH solution was significantly enhanced in the presence of Zn(II) (Figure 1A), with the λ_{Em} detected at 490 nm (Ex: 395 nm) (Figure 1B) and τ of 4.63 ns (Table 1). Simultaneously, the photoluminescence efficiency was improved, with an enhanced QY of 15% for cyclo-HH + Zn(II) (Table 1). The emission of the cyclo-HY solution was also enhanced to some extent in the presence of Zn(II), with the λ_{Em} detected at 490 nm (Ex: 380 nm) (Figure S5, Supporting Information), τ of 4.79 ns and a QY of 9% (Table 1), similarly to cyclo-WW, as we have previously published.[31] In contrast, the other dipeptides did not show any noticeable changes in the presence of Zn(II) (Figures S6 and S7, Supporting Information).

Since the most effective enhancement was observed for cyclo-HH, we next focused on studying the cyclo-HH self-assembly process, and specifically the very initial nucleation stage, in the absence or presence of Zn(II), in order to elucidate the mechanism underlying the metal ion doping mediated photoluminescence improvement. AFM characterizations demonstrated that only dot-like nanoparticles, several nanometers in height, were present in the cyclo-HH + Zn(II) solution (Figure 1C). Accordingly, dynamic light scattering (DLS) experiments revealed that the dominant particles in the solutions were only several

nanometers size, compared to dozens to hundreds of nanometers for the same peptides in the absence of zinc ions (Figure 1D). These results indicated that the coordination with Zn(II) inhibited the hierarchical organization of cyclo-HH, resulting in separation of the oligomers from each other, thereby leading to their stabilization.

2.3 Conformational Alternation Upon Zinc Ions Coordination

Fourier-transform infrared spectroscopy (FTIR) analysis indicated that after Zn(II) coordination, the −NH stretching vibration peaks of the cyclo-HH became narrower and sharper, indicating that less hydrogen bonds were formed and many −NH moieties remained free. In addition, the insert backbone C–C stretching vibration peaks became relatively stronger, indirectly confirming that the active nitrogen atoms extensively participated in complexation with Zn(II) and the coordination distinctly hindered the IR absorption of the relevant chemical bonds.[31] This confirmed that the active nitrogen atoms extensively participated in complexation with Zn(II) (Figure S8, Supporting Information),[43] as we previously demonstrated for cyclo-WW + Zn(II).[31]] ^{1}H NMR was then utilized to study the mechanism underlying the complexation between peptides and metal ions. The chemical shifts ($\Delta\delta$) of cyclo-HH hydrogen atoms revealed band broadening along with upfield shifting following coordination with Zn(II) (Figure 2A,B), especially for the imine protons of the side-chain imidazole ring (marked with *b*, $\Delta\delta$ = 0.11 ppm) (Figure 2C), indicating that the shielding effect of the electron clouds had become stronger. The results suggest that the imidazole ring, rather than the diketopiperazine rings in the cyclo-WW + Zn(II) case,[31] coordinated with Zn(II) through the imine nitrogen atom, thus decreasing the attraction of electrons outside the proton at the *b* position. Combining these findings, we hypothesize that the molecular configurations of the cyclo-HH molecules are different in the absence and in the presence of zinc ions.

Molecular dynamics (MD) simulations were further utilized to study the self-assembly of cyclo-HH. Across all simulations, visual inspection confirmed that highly disordered clusters of cyclodipeptides deformed and reformed, ensuring that the cyclodipeptides were not trapped in a local energetic minimum in a given simulation, while facilitating the formation of structures with higher order or symmetry (data not shown). First, we focused on the formation of the elementary interactions between a pair of cyclodipeptide molecules resulting in an ordered structure. In the cyclo-HH methanol solution, cyclo-HH dipeptides tended to form ordered conformations where both imidazole side chains were located on the same side of the backbone diketopiperazine rings, namely “Class 1” β-bridge like conformation (Figure 2D, left panel; Table S1, Supporting Information). In contrast, in the cyclo-HH + Zn(II) system, pairs of cyclo-HH dipeptides tended to form ordered conformations such that the imidazole side chains of the two interacting dipeptides were on the opposite sides of the backbone, namely “Class 2” β-bridge like conformation (Figure 2D, right panel; Table S2, Supporting Information), as also confirmed by subsequent crystallographic characterization following the hierarchically oriented organization principle (data not shown).[7,21] The “Class 2” β-bridge like conformations were primarily observed only if Zn(II) was coordinated between two H imidazole rings belonging to opposite, β-bridge bonded cyclo-HH dipeptides (Figure 2D). Otherwise, if the pair of cyclo-HH dipeptides was not coordinated with Zn(II), the molecules tended to form “Class 1” β-bridge

like conformations (Table S3, Supporting Information). These findings indicate that the introduction of Zn(II) indeed affected the association of cyclo-HH dipeptides and that the "Class 2" β-bridge like conformation was stabilized by Zn(II) through "locking" the pair of cyclo-HH molecules. These β-bridge like dimeric conformations are probably the basic units that act as the building blocks to self-assemble into clusters and subsequently into larger crystals,[36] thus implying the structural basis underlying the photoactive properties. In contrast, in the cyclo-HY + Zn(II) system, which showed weaker photoluminescence enhancement compared to cyclo-HH + Zn(II), the Zn(II) ions did not steer any conformational alternations, with both conformation types formed at a nearly equal proportion (Figure S10, Table S4, Supporting Information). In addition, the Zn(II) was primarily coordinated with only one H of two bonded cyclo-HY molecules independent of which class the dipeptide adopted, in contrast to the cyclo-HH + Zn(II) system where Zn(II) was coordinated with two H residues of opposing "Class 2" β-bridge bonded dipeptides (Figure 2D).

Interestingly, the ordered β-bridge like conformations of cyclo-HH mostly coexisted with relatively amorphous structures of cyclo-HH arranged in larger clusters (Tables S1, S2, and S3, Supporting Information), with the ordered conformations positioned in the core and the amorphous layers partially surrounding in the perimeter (Figure 3), reminiscent of pseudo "core/shell" architectures. According to our additional calculations, the outer amorphous layers can provide a stabilizing environment for the core ordered structures, thereby improving their durability. Notably, this type of architecture can stabilize the dots, thus enhancing the QY and the photoluminescence intensity.[44]

Within the clusters of cyclo-HH + Zn(II), the ratio of Zn(II) to cyclo-HH dipeptide was higher in the core (0.5–1.13) than in the shell layers (0.42–0.82) (Table S5, Supporting Information). The ratio of Zn(II) to cyclo-HH dipeptide is approximately 1:1 for two adjacent cyclo-HH molecules, while the ratio of Zn(II) to chloride ions is approximately 1:2 (Table S5, Supporting Information), thus indicating that the Zn(II) involved in "Class 2" β-bridge like conformations is coordinated with two imidazole rings of cyclo-HH dipeptide pairs along with the two chloride ions. The Zn(II) to cyclo-HH ratio was lower for the clusters comprising more adjacent peptides, while keeping the ratio of Zn(II) to chloride ions consistent (Table S5, Supporting Information). Nevertheless, elongated β-bridge like conformations comprising a 1:1 ratio of Zn(II) to cyclo-HH could still be observed. An example of a cluster containing seven cyclo-HH dipeptides and four Zn(II) ions is shown in Figure 3, where four adjacent cyclo-HH monomers formed an elongated "Class 2" β-bridge like conformation by coordinating with four Zn(II) ions at a 1:1 ratio (Figure 3D, dark blue region). For comparison, the ratio of Zn(II): cyclo-HY was less than 1:3 (Table S6, Supporting Information), notably lower than the 1:1 ratio observed for cyclo-HH + Zn(II). Additionally, the ratio of Zn(II): cyclo-HY did not differ in the core of the clusters versus the shell layers. These structural differences between cyclo-HH and cyclo-HY in the presence of Zn(II) suggest that the emission of the cyclodipeptide assemblies is influenced by their ability to coordinate with Zn(II). The presence of two H within cyclo-HH could allow for the Zn(II) ions to "lock" in elongated "Class 2" β-bridge like conformations, which finally enhanced the QY of the assemblies.

Europe PMC Funders Author Manuscripts

Additional statistical analysis further focused on the structural and energetic properties of cyclo-HH self-assembly in the presence of Zn(II). Statistical analysis of all instances of cyclo-HH "Class 2" β-bridge like conformations, irrespective of whether the pair of cyclo-HH was within a larger cluster or not, showed that the Zn(II) ion first coordinated with the H of one cyclo-HH dipeptide (Figure 2Ei). Then, the H of a second cyclo-HH monomer coordinated with the Zn(II) to form a dimer, at a statistical proportion of 47.2% (Figure 2Eii). Following the coordination, the two cyclo-HH monomers began to form hydrogen bond interactions between their backbone atoms (Figure 2Eiii), at a statistical proportion of 49.2%, to finally form β-sheet bridge-like configurations at a statistical proportion of 83.1% (Figure 2Eiv). The relatively low instances of the first two stages (<50%) indicate that a large proportion of cyclo-HH monomers remained separated in the solution, consistent with the DLS results. This analysis suggests that Zn(II) was not coordinated with preformed peptide structures, but rather drove the formation of the "Class 2" β-bridge like conformations following attraction to the peptide monomers at the very early stage of the assembly process. The aforementioned analysis focused on the Zn(II) ion simultaneously shared by two H side-chains. However, during the simulations, an additional Zn(II) ion was commonly present within the "Class 2" β-bridge like conformations, such that it was coordinated with one of the remaining H side-chains of the two β-bridge bonded cyclo-HH dipeptides. This is indicated by the ≈1:1 ratio of Zn(II) to cyclo-HH in the "Class 2" β-bridge like conformations comprising two adjacent peptides (Table S5, Supporting Information).

2.4 "Environment-Switching" Doping Mechanism of the Metal Ions

Free energy calculations were further performed to elucidate the driving forces leading to the formation of clusters in the cyclo-HH + Zn(II) system. Upon the formation of clusters, the two entities were strongly attracted at an average of −10.0 kcal mol^{-1} per peptide, primarily due to polar attraction interactions (Figure S11A, Supporting Information). The formation of such clusters did not result from association of preformed assemblies of cyclo-HH and Zn(II), as depicted by an average unfavorable association free energy of 2.8 kcal mol^{-1} per peptide (Figure S11B, Supporting Information), thus confirming the previous conclusion that Zn(II) ions play an essential role in the dynamics of association to form "Class 2" β-bridge like conformations. This can be further reflected by the free energy of cyclo-HH dipeptide association in the absence of Zn(II) (-6.7 kcal mol^{-1} per peptide), which was lower than in the presence of Zn(II) (−5.7 kcal mol^{-1} per peptide), with the contribution of Zn(II) neglected (Figure S11C, Supporting Information).

We next aimed to obtain further insights into the mechanism underlying the contribution of Zn(II) to the association of cyclo-HH. Assuming that all the assembling entities were immersed in the solvent prior to association, the calculated average association free energy per peptide was −0.7 kcal mol^{-1} (Figure S11D, Supporting Information), considerably less favorable than the corresponding energy when neglecting the contribution of Zn(II) (−5.7 kcal mol^{-1} per peptide). Therefore, for the association to be thermodynamically driven, Zn(II) should be first surrounded by a lower dielectric environment. Finally, we recalculated the average association free energy assuming that Zn(II) ions were surrounded by the lower dielectric environment provided by the dipeptides prior to assembly. The resulting value,

Europe PMC Funders Author Manuscripts

−14.8 kcal mol^{-1} per peptide (Figure S11E, Supporting Information), indicates a strong energetically favorable association, primarily resulting from the polar solvation free energy component. Thus, it could be concluded that the doping of cyclo-HH association by Zn(II) is initially driven by a relatively small energetic penalty for the transfer of Zn(II) to a lower dielectric medium, counterbalanced by single or pairs of cyclo-HH monomers attracting and pulling Zn(II) from the solvent to the peptide-rich environment, thus comprising an "environment-switching" mechanism (Figure 3). This mechanism could be observed within MD simulations, with Zn(II) first coordinated with cyclo-HH monomers (Figure 3B), promoting their self-assembly (Figure 3C) into pseudo "core/sell" clusters (Figure 3D).

2.5 Bioinspired Light Emitting Diode Using Peptides Assemblies as Phosphors

The photoluminescent nature makes the bioinspired self-assemblies interesting candidates for ecofriendly optoelectronic applications.[45] By combining a mixture of dried cyclo-HH + Zn(II) dots and polydimethylsiloxane with a 420 nm emissive InGaN chip, a prototypical light emitting diode (LED) device using peptide self-assemblies as phosphors was fabricated. As shown in Figure 4A, bright green light with an emission around 565 nm (Figure 4B) was obtained when the LED operated under voltage of 3.0 V, with Commission Internationale de L'Eclairage (CIE) coordinates of (0.37, 0.40) and a color temperature of 4415 K (Figure 4C). As a control, a LED comprising cyclo-HH alone showed the intrinsic blue emission of the chip (Figure S9, Supporting Information), thus confirming the requirement of Zn(II) for enhanced green photoluminescence. These results demonstrate that the aromatic cyclodipeptide self-assembling photoactive structures show a promising prospect for use in the ecofriendly optoelectronic field, potentially bridging between the optical world and biological systems.

3 Conclusion

By thorough analysis of aromatic cyclodipeptide self-assembly, we were able to demonstrate the enhancement of fluorescence via coordination with Zn(II). The combined Zn(II) and cyclo-HH assembly is energetically favorable through the initiation of interactions between the ions and peptides, allowing Zn(II) to be initially attracted and pulled from the solvent into a peptide-rich low dielectric environment. This mechanism can lead to the formation of the higher-complexity ordered structures and is termed "environment-switching" doping. As such, the initial nucleation process is presumably dynamic, where Zn(II) and peptides gradually and synergistically contribute to self-assembly.[46] Specifically, based on our simulations and free energy calculations, the process is driven by a continuous complexation of Zn(II) mainly to the ordered Zn(II)-triggered conformations and, to a lesser extent, to the amorphous peptide aggregate layers. The peptides from the amorphous layer could coalesce into the ordered structures, thus resulting in clusters growth. In parallel, the amorphous layers can facilitate the formation of multicomponent cyclo-HH + Zn(II) assemblies, as the energetic penalty for ion transfer from the methanol into a peptide-rich low dielectric environment can be counterbalanced by interactions between cyclo-HH and Zn(II), thereby favoring the subsequent formation of ordered structures. These bioinspired photoactive supramolecular structures could be used as bio-organic phosphors for the fabrication of ecofriendly lighting devices. Aiming to further exploit their potential for such applications,

diverse modulation strategies, such as the design of larger cyclooligopeptides, substitution with other side-chains, complexation with other metal ions, flexible assembly approaches, self-assembly in different solvents etc., can be employed to tune the cyclopeptides self-assembly. This may result in diverse supramolecular structures with a rainbow of photoluminescence in the visible and even infrared region. With these goals achieved, aromatic peptide self-assemblies can be expected to serve as a new type of bio-organic, supramolecular photoluminescent materials to complement the currently used state-of-the-art counterparts.

This combined theoretical and experimental study provides, for the first time, insights into the mechanism and driving forces leading to the doping of biomolecules by metal ions, thus elucidating the very first stages of self-assembly prior to the formation of highly-ordered structures. Importantly, the resulting architectures and the doping mechanism can be utilized as useful tools for further molecular design and virtual screening for advanced optoelectronic applications in similar systems. In addition, our studies suggest that such systems composed of small peptides can be used as models to provide insights into the role of metal ions in self-assembly, potentially also applicable for the in vivo organization of larger polypeptides or proteins.

4 Experimental Section

Materials

Aromatic cyclodipeptides were purchased from Bachem (Bubendorf, Switzerland), DGpeptides (Hangzhou, China) or GL Biochem (Shanghai, China). Zinc chloride ($ZnCl_2$), anhydrous MeOH, and deuterated methanol (MeOH-d_4) were purchased from Sigma Aldrich (Rehovot, Israel). All materials were used as received without further purification. Water was processed using a Millipore purification system (Darmstadt, Germany) with a minimum resistivity of 18.2 MΩ cm. Polydimethylsiloxane (PDMS) elastomer kits (Sylgard 184) were purchased from Dow Corning (Midland, MI, USA). 420 nm emissive InGaN chips (emission peak at 420 nm, operation under voltage of 3.0 V) were purchased from Greatshine Semiconductor Technology Co. Ltd.

Sample Preparation

Cyclodipeptides were added to anhydrous MeOH or MeOH solutions of $ZnCl_2$ to final concentrations of 5.0×10^{-3} M cyclodipeptides and 10.0×10^{-3} M metal salts, when used. To dissolve the peptides, the solutions were incubated in an 80 °C water bath for 5 min, after which most of the solutions became transparent.

Atomic Force Microscopy

4 μL of sample solution was dropped onto a freshly cleaved mica surface and was allowed to air dry. The mica was then rinsed with water and gently purge dried with nitrogen. A topographic image was recorded under a NanoWizard 3 BioScience AFM (JPK, Berlin, Germany) in the tapping mode at ambient temperature, with a 512 × 512 pixel resolution and a scanning speed of 1.0 Hz.

Fluorescence

600 μL sample solution was pipetted into a 1.0 cm path-length quartz cuvette, and the spectrum was collected using a FluoroMax-4 Spectrofluorometer (Horiba Jobin Yvon, Kyoto, Japan) at ambient temperature. The excitation and emission wavelengths were set at 300–450 and 380–600 nm, respectively, with a slit of 3 nm. According to the samples, anhydrous MeOH or MeOH solution of $ZnCl_2$ was used as background and subtracted.

Quantum Yield Measurement

5 mL sample solution was pipetted into a 1.0 cm path-length quartz cuvette with a tube (Hellma, Müllheim, Germany), and the absolute QY was measured on an absolute PL quantum yield spectrometer C11347 (Hamamatsu Photonics, Shizuoka, Japan) at ambient temperature. The relevant solvents, namely anhydrous MeOH or MeOH solution of $ZnCl_2$, were used as background and subtracted. At least five measurements were performed and averaged for accuracy.

Fluorescent Decay Measurement (Lifetime)

600 μL sample solution was pipetted into a 1.0 cm path-length quartz cuvette, and the spectrum was collected using a FluoroMax-4 Spectrofluorometer (Horiba Jobin Yvon, Kyoto, Japan) equipped with a NanoLED laser excitation source at ambient temperature. The wavelength was set to the maximal excitation and emission of the samples, and a LUDOX sample (silica beads, 2 μm) was used as the prompt. The lifetime was determined by fitting the fluorescent decay data from the DAS6 Analysis software (Horiba Jobin Yvon, Kyoto, Japan). Three measurements were performed and averaged for accuracy.

Nuclear Magnetic Resonance

Cyclo-HH or cyclo-HH + Zn(II) were dissolved in MeOH-d_4 with tetramethylsilane as the internal standard to a final concentration of 5.0×10^{-3} M dipeptide and 10.0×10^{-3} M Zn(II), when used. ^{1}H NMR spectra were recorded on a Bruker AV-400 NMR spectrometer with chemical shifts reported as ppm. The difference in the chemical shift values before and after the addition of Zn(II) into the cyclo-HH solution ($\Delta\delta = \delta_{\text{cyclo-HH}} - \delta_{\text{cyclo-HH + Zn(II)}}$) was calculated in ppb and plotted as a function of amide, aromatic and aliphatic protons.

Dynamic Light Scattering

850 μL of the sample solution was introduced into a DTS1070 folded capillary cell (Malvern, Worcestershire, UK), and the size was measured using a Zetasizer Nano ZS analyzer (Malvern Instruments, Malvern, UK) at 25.0 °C and a backscatter detector (173°). Three measurements were performed and averaged for accuracy.

Fourier Transform Infrared Spectroscopy

750 μL of the sample solution was dropped onto polyethylene IR card (International Crystal Labs, Garfield, NJ, USA) and air dried. The FTIR spectra were recorded on a Nicolet 6700 FTIR spectrometer (Thermo Scientific, Waltham, MA, USA), from 4000 to 400 cm^{-1} at room temperature. 128 scans were collected with a spectral resolution of 4 cm^{-1} in nitrogen

Europe PMC Funders Author Manuscripts

atmosphere. The corresponding reference spectra (anhydrous MeOH or MeOH solution of $ZnCl_2$) were recorded under identical conditions and subtracted.

Theoretical Calculations of Molecular Orbital Amplitudes and Energy Levels

Density functional theory calculations were carried out based on the self-consistent solution of Kohn-Sham function and the projector augmented wave pseudopotential as implemented in the Vienna Ab-initio Simulation Package (VASP).

The exchange-correlation potential was in the form of Perdew-Burke-Ernerhof (PBE) with generalized gradient approximation (GGA). For the structural relaxation, the energy convergence threshold was set to 10^{-5} eV and the residual force on each atom was less than 0.03 eV $Å^{-1}$. The cut-off energy for the plane-wave basis was set to 500 eV. To eliminate interactions between the molecule and its periodic images, a vacuum distance larger than 15 Å for each direction in the supercell geometry was used.

Molecular Dynamics Simulations and Free Energy Calculations: Modeling and Simulations

MD simulations were performed to investigate the self-assembly properties of three systems comprising cyclo-HH dipeptides, cyclo-HH dipeptides + Zn(II), and cyclo-HY dipeptides + Zn(II) in MeOH. Five MD simulation production runs were performed for each system. The duration of each run was 200 ns. All energy minimization and MD simulations were performed using the CHARMM36 force field, a Drude polarizable force field and periodic boundary conditions in CHARMM. Upon completion of the MD simulations, the five independent simulation trajectories were merged, resulting in a total of 5000 snapshots analyzed per system. The analysis was focused on elucidating the key interactions between cyclodipeptides in the absence or presence of Zn(II), and on uncovering the key driving forces leading to self-assembly. The details on the MD simulations are provided in the Supporting Information.

Characterization of the Interactions between Pairs of Cyclodipeptide Monomers, and between Cyclodipeptide and Zn(II)

During the simulations, the gradual formation of clusters by cyclodipeptides was observed, which can potentially correspond to the structures formed in the first instances of association. The clusters were defined to be formed by interactions between cyclodipeptides as well as between cyclodipeptides and Zn(II) for the simulated systems. Distance cutoffs were used to define the interactions between two cyclodipeptide monomers as well as between cyclodipeptides and Zn(II). These distance criteria are detailed in the Supporting Information. FORTRAN programs were developed to detect elementary structures comprising two interacting cyclodipeptides, based on the distance cutoffs. The elementary structures were then integrated to into clusters, such that a number of n cyclodipeptides were defined to form a cluster when each dipeptide was in the vicinity of at least another one based on any of the distance criteria defined in Supporting Information. The ratio of Zn(II) to cyclodipeptide within each cluster was additionally determined based on the distance criteria defined in Supporting Information.

Europe PMC Funders Author Manuscripts

The criteria were further used to identify the ordered structures and the amorphous conformations, which could either be isolated entities, or entities within clusters; the latter is of particular interest in our analysis. Cyclodipeptides interacting through their backbone N or O atoms were classified as ordered β-bridge like conformations and cyclodipeptides interacting through any other interactions were classified as amorphous conformations. In a given simulation snapshot, a number of n cyclodipeptides were defined to form an elongated β-bridge like conformation when each dipeptide monomer formed backbone interactions with at least another. It should be noted that the ordered β-bridge like conformations of 2-, 3-, or 4- (the maximum observed) adjacent cyclo-HH dipeptides were observed either as independent entities (i.e., as clusters comprising 2, 3, and 4 dipeptides, respectively) or within larger clusters, coexisting with the amorphous structures.

Structural and Energetic Analysis of Clusters Formed by Cyclo-HH in the Absence or Presence of Zn(II)

Structural analysis was used to identify the pathways leading to the formation of ordered structures coordinating with Zn(II) in comparison to structures in the absence of Zn(II). Additionally, interaction and association free energy calculations were performed using the MM-GBSA approximation to investigate the mechanism and driving forces leading to the association and stabilization of cyclo-HH dipeptides and Zn(II) within the clusters, in the first moments of self-assembly prior to the formation of highly ordered structures. Each calculation was performed for each individual cluster within the simulations; the resulting energy values were normalized by the number of cyclo-HH dipeptides within the cluster and decomposed into polar and nonpolar components. The methods used for the energy calculations are described in detail in the Supporting Information.

Fabrication and Characterization of LEDs

Commercially available InGaN chips were used at the bottom of the LED base. For the preparation of the color conversion layer, the cyclo-HH + Zn(II) MeOH solution was purge dried using ultrapure nitrogen, and then mixed with PDMS at a mass ratio of 1:1. The mixtures were applied on the InGaN chips and following curing at 80 °C for 1 h, the LEDs peptide phosphors were obtained.

Supplementary Material

Refer to Web version on PubMed Central for supplementary material.

Acknowledgements

K.T., Y.C., and A.A.O. contributed equally to this work. This work was supported in part by the European Research Council under the European Union Horizon 2020 research and innovation program (No. 694426) (E.G.,), Joint NSFC-ISF Grant (no. 3145/19) (E.G.,), National Natural Science Foundation of China (No. 11874189) (M.S.S.), Texas A&M University Graduate Diversity Fellowship from the TAMU Office of Graduate and Professional Studies (A.A.O), and start-up funding by the Artie McFerrin Department of Chemical Engineering at Texas A&M University (P.T.). All MD simulations and free energy calculations were conducted using the Ada supercomputing cluster and additional computational resources available to P.T. at the Texas A&M High Performance Research Computing Facility and the Chemical Engineering Department. The authors thank Dr. Miri Kazes for QY experimental assistance and the members of the Tamamis and Gazit laboratories for helpful discussions.

References

[1]. Günes S, Neugebauer H, Sariciftci NS. Chem Rev. 2007; 107:1324. [PubMed: 17428026]

[2]. Pansieri J, Josserand V, Lee S-J, Rongier A, Imbert D, Sallanon MM, Kövari E, Dane TG, Vendrely C, Chaix-Pluchery O. Nat Photonics. 2019; 13:473.

[3]. Facchetti A. Mater Today. 2007; 10:28.

[4]. Wang CL, Dong HL, Jiang L, Hu WP. Chem Soc Rev. 2018; 47:422. [PubMed: 29186226]

[5]. Lampel A, McPhee SA, Park H-A, Scott GG, Humagain S, Hekstra DR, Yoo B, Frederix PWJM, Li T-D, Abzalimov RR, Greenbaum SG, et al. Science. 2017; 356:1064. [PubMed: 28596363]

[6]. Gazit E. Nat Nanotechnol. 2016; 11:309. [PubMed: 26751168]

[7]. Yuan C, Ji W, Xing R, Li J, Gazit E, Yan XH. Nat Rev Chem. 2019; 3:567.

[8]. Głowacki ED, Coskun H, Blood-Forsythe MA, Monkowius U, Leonat L, Grzybowski M, Gryko D, White MS, Aspuru-Guzik A, Sariciftci NS. Org Electron. 2014; 15:3521. [PubMed: 25642158]

[9]. Yan XH, Zhu PL, Li JB. Chem Soc Rev. 2010; 39:1877. [PubMed: 20502791]

[10]. Wang J, Liu K, Xing RR, Yan XH. Chem Soc Rev. 2016; 45:5589. [PubMed: 27487936]

[11]. Wang M, Zhou P, Wang JQ, Zhao YR, Ma H, Lu JR, Xu H. J Am Chem Soc. 2017; 139:4185. [PubMed: 28240550]

[12]. Tao K, Makam P, Aizen R, Gazit E. Science. 2017; 358:eaam9756. [PubMed: 29146781]

[13]. Erwin SC, Zu L, Haftel MI, Efros AL, Kennedy TA, Norris DJ. Nature. 2005; 436:91. [PubMed: 16001066]

[14]. Li Y, Zhao Y, Cheng H, Hu Y, Shi G, Dai L, Qu L. J Am Chem Soc. 2012; 134:15. [PubMed: 22136359]

[15]. Kim G-H, Shao L, Zhang K, Pipe KP. Nat Mater. 2013; 12:719. [PubMed: 23644522]

[16]. Pfeiffer M, Leo K, Zhou X, Huang JS, Hofmann M, Werner A, Blochwitz-Nimoth J. Org Electron. 2003; 4:89.

[17]. Lüssem B, Riede M, Leo K. Phys Status Solidi A. 2013; 210:9.

[18]. Polshakov VI, Mantsyzov AB, Kozin SA, Adzhubei AA, Zhokhov SS, Beek Wv, Kulikova AA, Indeykina MI, Mit-kevich VA, Makarov AA. Angew Chem, Int Ed. 2017; 56

[19]. Katsoulidis AP, Antypov D, Whitehead GFS, Carrington EJ, Adams DJ, Berry NGGR, Darling MSD, Rosseinsky MJ. Nature. 2019; 565:213. [PubMed: 30626943]

[20]. Laws K, Bineva-Todd G, Eskandari A, Lu C, O'Reilly N, Suntharalingam K. Angew Chem, Int Ed. 2018; 57:287.

[21]. Yuan C, Levin A, Chen W, Xing R, Zou Q, Herling TW, Challa PK, Knowles TPJ, Yan XH. Angew Chem, Int Ed. 2019; 58

[22]. Faller P, Hureau C, Berthoumieu O. Inorg Chem. 2013; 52

[23]. Dong J, Canfield JM, Mehta AK, Shokes JE, Tian B, Childers Seth W, Simmons JA, Mao Z, Scott RA, Warncke K. Proc Natl Acad Sci USA. 2007; 104

[24]. Dong J, Shokes JE, Scott RA, Lynn DG. J Am Chem Soc. 2006; 128:3540. [PubMed: 16536526]

[25]. Xing R, Zou Q, Yuan C, Zhao L, Chang R, Yan XH. Adv Mater. 2019; 31

[26]. Li Y, Zou Q, Yuan C, Li S, Xing R, Yan XH. Angew Chem, Int Ed. 2018; 57:17084.

[27]. Barondeau DP, Kassmann CJ, Tainer JA, Getzoff ED. J Am Chem Soc. 2002; 124:3522. [PubMed: 11929238]

[28]. Fan Z, Sun L, Huang Y, Wang Y, Zhang MJ. Nat Nanotechnol. 2016; 11:388. [PubMed: 26751169]

[29]. Lee M, Wang T, Makhlynets OV, Wu Y, Polizzi NF, Wu H, Gosavi PM, Stöhr J, Korendovych IV, DeGrado WF. Proc Natl Acad Sci USA. 2017; 114:6191. [PubMed: 28566494]

[30]. Noy D, Solomonov I, Sinkevich O, Arad T, Kjaer K, Sagi I. J Am Chem Soc. 2008; 130:1376. [PubMed: 18179213]

[31]. Tao K, Fan Z, Sun L, Makam P, Tian Z, Ruegsegger M, Shaham-Niv S, Hansford D, Aizen R, Pan Z. Nat Commun. 2018; 9

[32]. Pinotsi D, Grisanti L, Mahou P, Gebauer R, Kaminski CF, Hassanali A, Kaminski Schierle GS. J Am Chem Soc. 2016; 138:3046. [PubMed: 26824778]

[33]. Zhang H, Zheng X, Xie N, He Z, Liu J, Leung NLC, Niu Y, Huang X, Wong KS, Kwok RTK. Am Chem Soc. 2017; 139

[34]. Vauthey S, Santoso S, Gong H, Watson N, Zhang SG. Proc Natl Acad Sci USA. 2002; 99:5355. [PubMed: 11929973]

[35]. Kumar M, Ing NL, Narang V, Wijerathne NK, Hochbaum AI, Ulijn RV. Nat Chem. 2018; 10:696. [PubMed: 29713031]

[36]. Amdursky N, Molotskii M, Gazit E, Rosenman G. J Am Chem Soc. 2010; 132

[37]. Hauser CA, Zhang SG. Nature. 2010; 468:516. [PubMed: 21107418]

[38]. Iwunze MO. J Photochem Photobiol, A. 2007; 186:283.

[39]. Held, P. B-T Instruments; Winooski, VT: 2003. https://www.biotek.com/resources/docs/Synergy_HT_Quantitation_of_Peptides_and_ Amino_Acids.pdf. [accessed: May 2018]

[40]. Maia FF Jr, Freire VN, Caetano EWS, Azevedo DL, Sales FAM, Albuquerque EL. J Chem Phys. 2011; 134

[41]. Zanatta G, Gottfried C, Silva AM, Caetano EWS, Sales FAM, Freire VN. J Chem Phys. 2014; 140

[42]. Sturala J, Etherington MK, Bismillah AN, Higginbotham HF, Trewby W, Aguilar JA, Bromley EHC, Avestro A-J, Monk-man AP, McGonigal PR. J Am Chem Soc. 2017; 139

[43]. Wang X, Pandey RR, Singh KV, Senthil Andavan GT, Tsai C, Lake R, Ozkan M, Ozkan CS. Nanotechnology. 2006; 17:1177.

[44]. Dabbousi BO, Rodriguez-Viejo J, Mikulec FV, Heine JR, Mattoussi H, Ober R, Jensen KF, Bawendi MG. J Phys Chem B. 1997; 101:9463.

[45]. Park S, Heo SW, Lee W, Inoue D, Jiang Z, Yu K, Jinno H, Hashizume D, Sekino M, Yokota T. Nature. 2018; 561:516. [PubMed: 30258137]

[46]. Micklitsch CM, Knerr PJ, Branco MC, Nagarkar R, Pochan DJ, Schneider JP. Angew Chem, Int Ed. 2011; 50:1577.

Europe PMC Funders Author Manuscripts

Europe PMC Funders Author Manuscripts

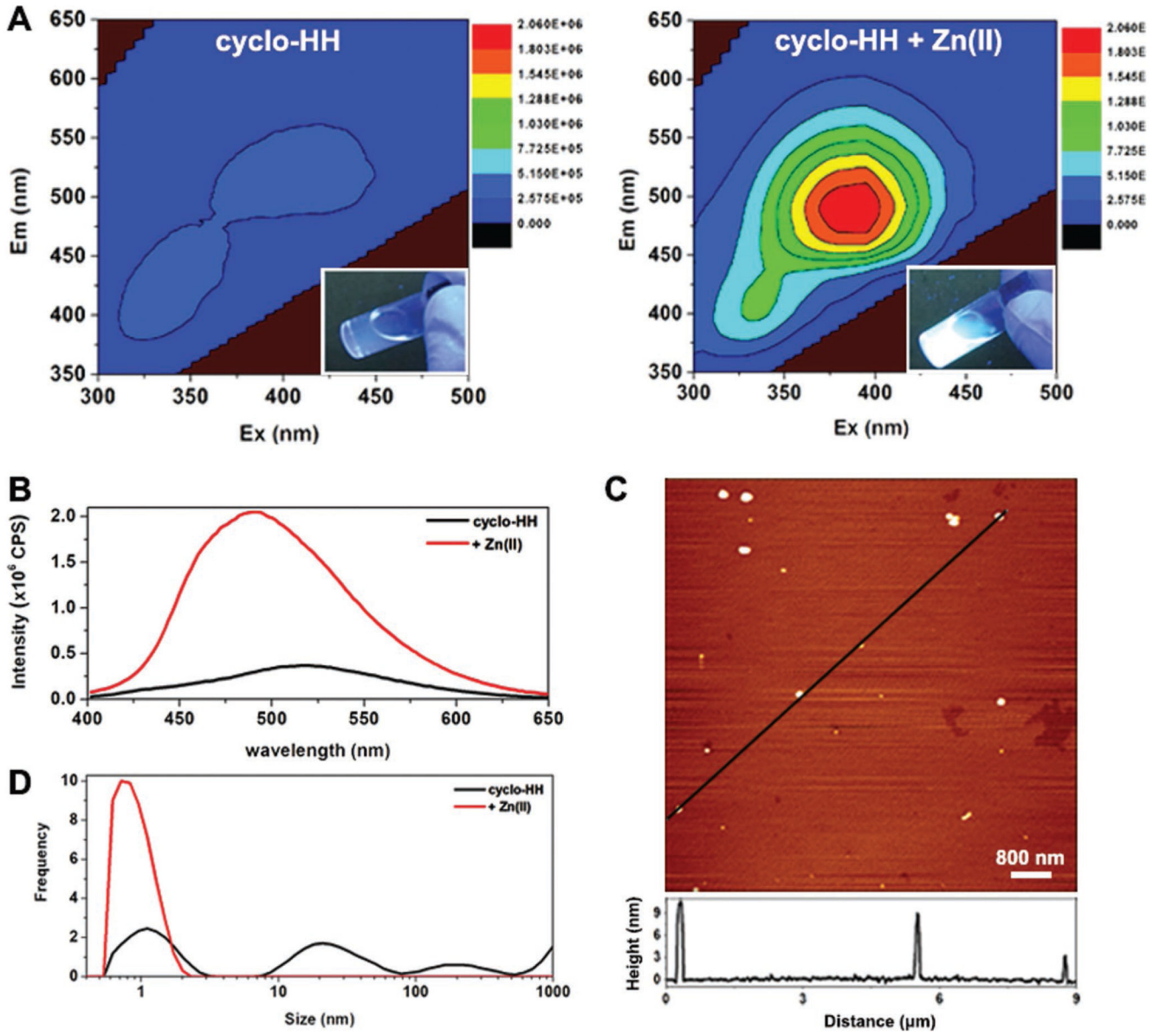

Figure 1.

Doping of cyclo-HH self-assemblies through coordination with Zn(II). A) Fluorescence contour profiles of cyclo-HH in the absence (left) or presence (right) of Zn(II). The contour profile of the peptide alone was extracted from Figure S4 (Supporting Information) for comparison. The insets show photographic pictures of the corresponding peptide solutions under UV light irradiation (365 nm). B) Extracted maximal emission spectra of cyclo-HH in the absence (black) or presence (red) of Zn(II) ions. C) AFM image of cyclo-HH + Zn(II). The height profile corresponds to the black line in the AFM image, showing dot-like nanoparticles of only several nanometers. D) DLS profile of cyclo-HH in the absence (black) or presence (red) of Zn(II) ions.

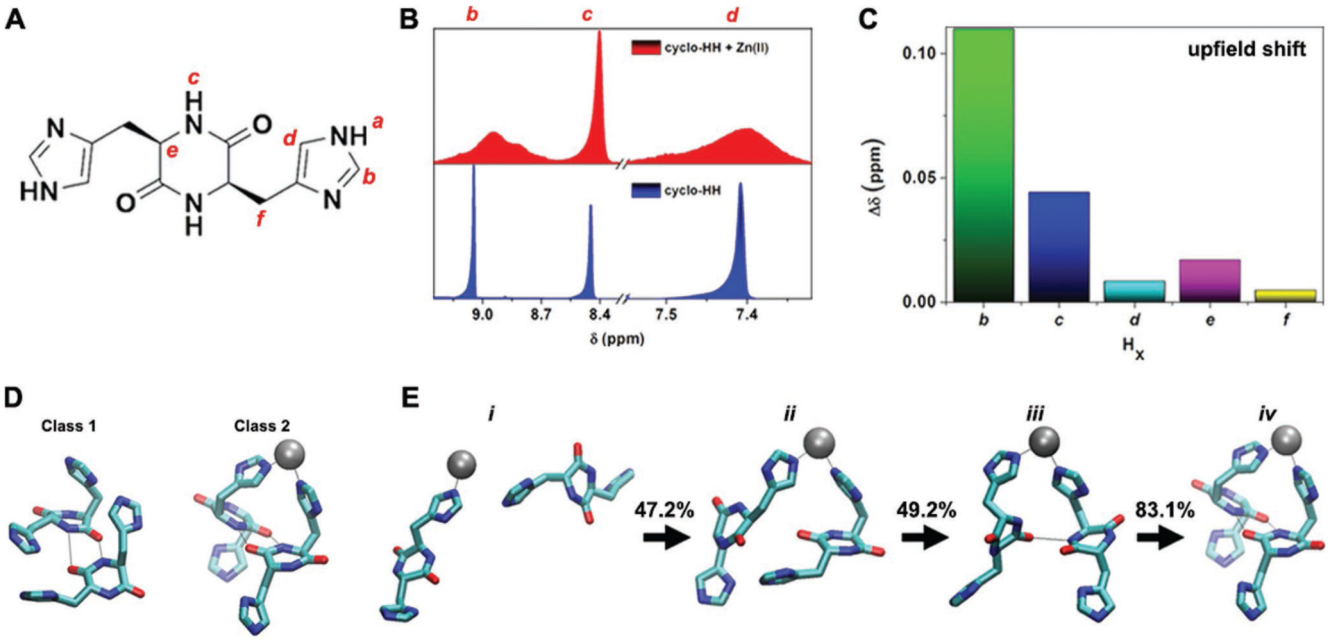

Figure 2.

Mechanistic analysis of cyclo-HH self-assembly doping by Zn(II). A) Molecular structure of cyclo-HH, with the hydrogen atoms in different chemical environments marked with italicized alphabet letters. B) ^{1}H NMR spectrum of cyclo-HH in the absence (blue) or presence (red) of Zn(II). C) Chemical shifts of hydrogen atoms upon doping with Zn(II), compared to the peptide alone. D) Graphic images of “Class 1” and “Class 2” β-bridge like conformations of cyclo-HH dimers. E) Graphic showing the self-assembly procedure of cyclo-HH + Zn(II) into “Class 2” β-bridge like conformations, with the frequency percentage shown above the arrows. Note that in D,E), the cyclo-HH molecules and Zn(II) ions are shown in licorice and gray van der Waals representations, respectively. Hydrogen bonds and Zn(II) coordination are indicated with thin black lines.

Europe PMC Funders Author Manuscripts

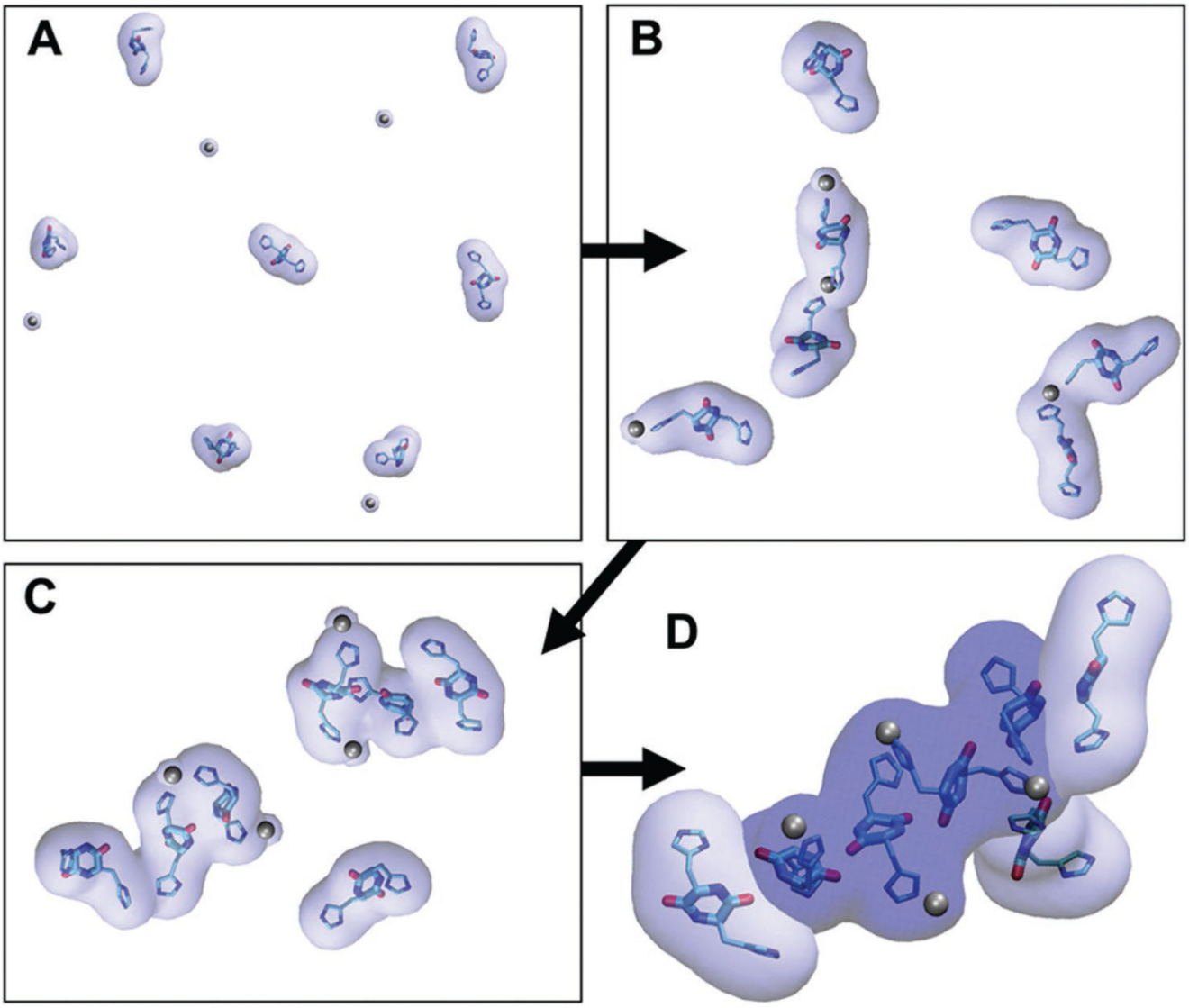

Figure 3.

Representative graphic images of the progression of cyclo-HH + Zn(II) self-assembly as detected by MD simulations and structural analysis softwares. A) Cyclo-HH and Zn(II) are initially dispersed in methanol. B) Zn(II) ions are then pulled from the methanol solvent into the peptide-rich environment of single or pairs of cyclo-HH, allowing C) the cyclo-HH-Zn(II) pairs to begin to self-assemble. D) Finally, cyclo-HH and Zn(II) form pseudo "core/shell" clusters. The cyclo-HH monomers forming the partly surrounding section of the cluster (amorphous layer, hereby denoted as "shell") are denoted with a light blue surface. The cyclo-HH monomers forming the elongated "Class 2" β-bridge like conformation (core region, hereby denoted as "core") are denoted with a dark blue color. The four cyclo-HH molecules forming the elongated "Class 2" β-bridge like conformation coordinate with four Zn(II) ions at a 1:1 ratio. Note that the cyclo-HH molecules and Zn(II) ions are shown in licorice and grey van der Waals representations, respectively.

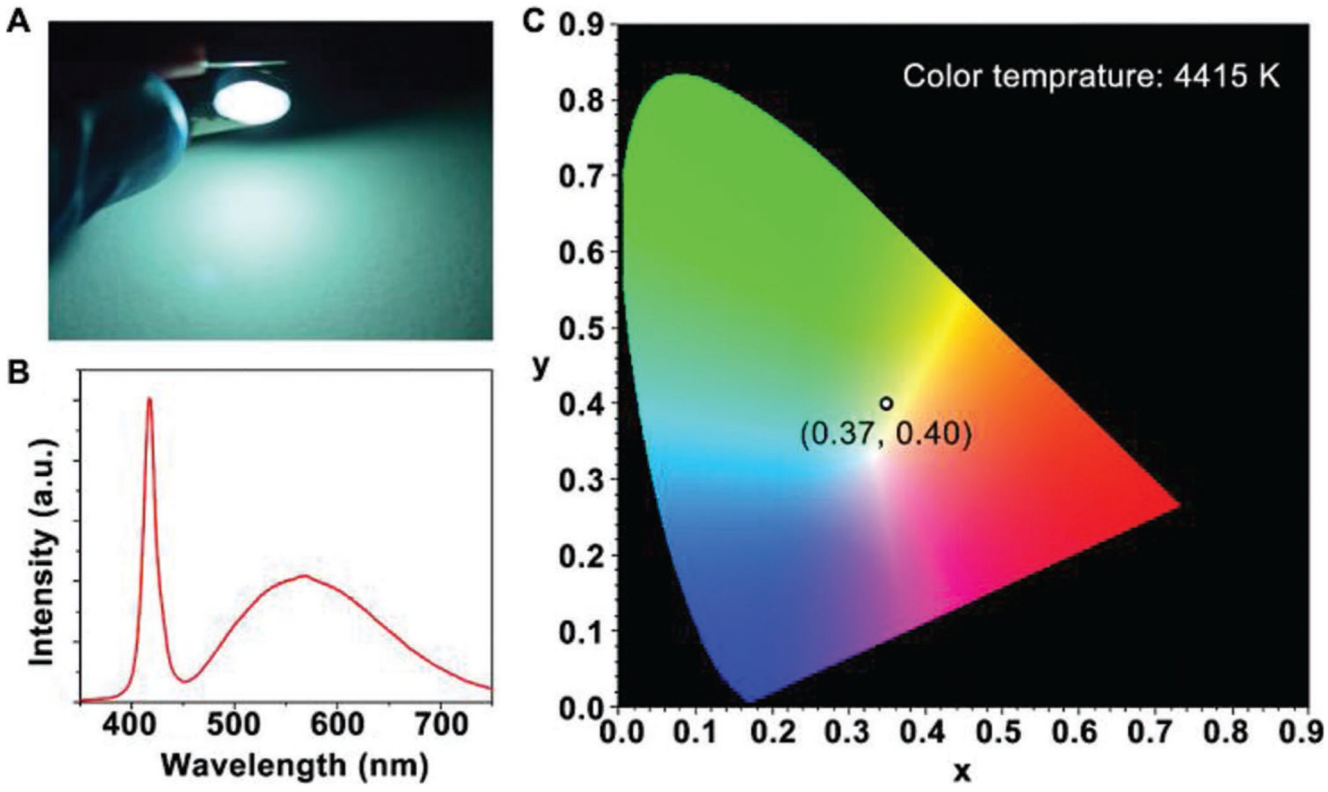

Figure 4.

Application of cyclo-HH + Zn(II) assemblies as phosphors for LED illumination. A) Photographic picture depicting the prototype, emitting bright green light upon excitation at 420 nm. B) Emission spectrum of the LED operated under a voltage of 3.0 V. C) CIE coordinates of the operating LED and the corresponding color temperature.

Europe PMC Funders Author Manuscripts

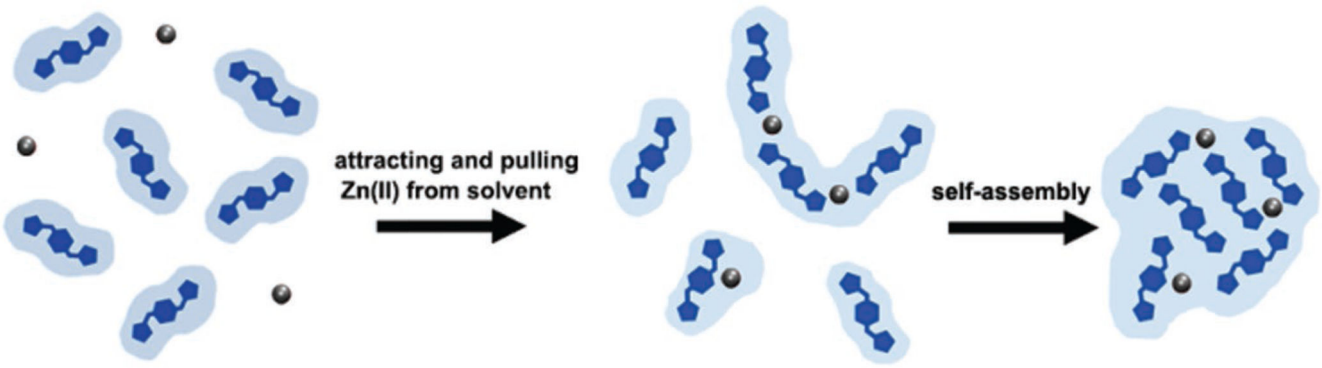

Scheme 1.

Schematic presentation of the “environment-switching” doping mechanism. The association of cyclodipeptides in the presence of Zn(II) is driven by single or small pairs of dipeptides initially attracting and pulling Zn(II) from the solvent, allowing Zn(II) to be in a more peptide-rich environment, and promoting their association into a cluster.

Europe PMC Funders Author Manuscripts

Europe PMC Funders Author Manuscripts

Table 1

Morphology and the corresponding fluorescence parameters of aromatic cyclodipeptide assemblies.

	ΔE [eV]	Structures	λ_{Ex} [nm]	λ_{Em} [nm]	QY[a)] [%]	τ [ns]
cyclo-HH	3.61	Nanofibers	340	425	3	4.89 ± 0.02
			420	520	7	6.48 ± 0.04
cyclo-YY	4.00	Platelets	–	–	–	–
cyclo-WW[31]	3.56	Nanospheres	370	440 (strong) 520 (weak)	2	5.45 ± 0.03
cyclo-FF	4.50	Nanofibers	–	–	–	–
cyclo-HY	4.00	Nanofibers	310	390	3	0.003 ± 0.034
cyclo-WH	3.56	Nanofibers	320	380 (strong)	3	0.07 ± 0.01
			370	465 (weak)	2	11.37 ± 0.05
cyclo-WY	4.55	Nanofibers	320	400	3	0.232 ± 0.004
cyclo-HF	4.19	Nanofibers	340	410	2	3.29 ± 0.03
cyclo-FY	3.94	Nanofibers	350	430	3	0.022 ± 0.003
cyclo-FW	3.63	Platelets	370	465	2	4.52 ± 0.05
cyclo-HH + Zn(II)	–	Nanodots	395	490	15	4.63 ± 0.01
cyclo-WW + Zn(II)[31]	–	Nanodots	370	520	11	3.63 ± 0.01
cyclo-HY + Zn(II)	–	Nanodots	380	490	9	4.79 ± 0.01

*a)*During QY measurements, due to the limitation of instrument parameters, the excitation was set to 350 nm if the maximal excitation wavelength of the samples was less than 350 nm.